Research Square

Preprints are preliminary reports that have not undergone peer review.
They should not be considered conclusive, used to inform clinical practice,
or referenced by the media as validated information.

Integrated Assessment of Soil, Airborne and External Gamma Radiation Indicators in Uranium Industry-Affected Areas of Uchkuduk, Uzbekistan

Umidjon Haydarov
xaydarovumid02@gmail.com

Samarkand State University named after Sharof Rashidov

Amrullo Muzafarov
Navoi State Mining and Technological University

Gulchehra Allaberganova
Navoi State Mining and Technological University

Mohinur Quvvatova
Navoi State Mining and Technological University

Guli Asadova
Navoi State Mining and Technological University

Sayyodjon Salimov
Navoi State University

Diyor Khazratov
Samarkand State University named after Sharof Rashidov

Research Article

Keywords: Uranium mill tailings, Radon progeny, Long-lived alpha activity, Ambient dose equivalent rate, Natural radionuclides, Uzbekistan

Posted Date: November 9th, 2026

DOI: https://doi.org/10.21203/rs.3.rs-11446355/v1

License: This work is licensed under a Creative Commons Attribution 4.0 International License. Read Full License

Additional Declarations: No competing interests reported.

Abstract

The soil radionuclide inventory, most often monitored in uranium industry areas, may not reflect the inhalation hazard. We tested this in Uchkuduk, Uzbekistan, at ten co-located points in each of a uranium sorption recovery section, a mill tailings site and the residential area, measuring ^{226}Ra, ^{232}Th and ^{40}K in soil, the radium equivalent activity (Ra_{eq}), the ambient dose equivalent rate $H^*(10)$, the equilibrium equivalent radon concentration (*EERC*) and the long-lived alpha activity (*LLAA*) of aerosols. The tailings site had the highest ^{226}Ra, Ra_{eq} and $H^*(10)$ (up to 5.85 μSv h^{-1}), but outdoor *EERC* and *LLAA* were no higher than at the sorption section, where indoor *EERC* reached 46 Bq m^{-3}. Outdoor *EERC* followed ^{226}Ra at the sorption section and in the residential area, whereas at the wind-exposed tailings site only *LLAA* did (ρ = 0.89–0.92). Airborne indicators should therefore be measured directly rather than inferred from soil and gamma surveys.

Introduction

In areas associated with the uranium industry, technogenic activity can alter the natural distribution of radionuclides, cause local accumulation of certain radionuclides, and consequently increase radiation exposure levels [1, 2]. Tailings and other residual materials generated by uranium mining and processing remain sources of radioactive impact for long periods of time [3]. The principal radionuclides occurring in the rocks, soils, waters, and atmospheric air of such areas are the radionuclides of the ^{238}U and ^{232}Th decay series, together with natural ^{40}K [4, 5]. Studies conducted at various uranium mining enterprises worldwide and at storage areas for radioactive wastes generated during long-term uranium mining have shown elevated ^{226}Ra activity, increased gamma radiation levels, and intensified radon-related radiation impacts in such areas. According to UNSCEAR [2], natural radiation sources account for the major part of the radiation dose received by humans, with a worldwide average annual effective dose of 2.4 mSv, varying between 1 and 10 mSv in some regions.

^{232}Th and ^{238}U in the technogenic wastes of the uranium industry undergo alpha decay and serve as the parent radionuclides of long radioactive decay chains [9]. Decay of ^{222}Rn produces short-lived progeny that attach to aerosol particles and, when inhaled, deposit in the respiratory tract and irradiate the lung tissue. Their concentration is expressed as the equilibrium equivalent radon concentration (*EERC*), i.e., the radon activity concentration in equilibrium with its short-lived progeny that has the same potential alpha energy concentration as the actual progeny mixture; *EERC* is therefore the key quantity for assessing radon-related inhalation doses [10, 11]. In uranium industry areas, airborne dust can additionally carry long-lived alpha emitters of the uranium series, such as ^{238}U, ^{234}U, ^{230}Th, ^{226}Ra and ^{210}Po. The long-lived alpha activity (*LLAA*) of airborne aerosols, measured after the short-lived radon and thoron progeny have decayed, is used as an integral indicator of this dust-borne inhalation hazard [12]. ^{210}Po, which also forms in the atmosphere from ^{222}Rn via ^{210}Pb, is a strong alpha emitter and contributes significantly to the internal dose upon inhalation [13, 14].

During the Soviet era, large-scale uranium mining and processing were carried out in Central Asian countries. These processes generated large volumes of technogenic radioactive waste, most of which persist today as uranium legacy sites. Because the natural radionuclides contained in these objects have the potential to disperse into the environment, interest in studies aimed at assessing their radiation status and degree of environmental impact has grown considerably in recent years [15]. Studies carried out in Kazakhstan have revealed higher spatial variability of radon concentration, gamma dose rate, and radiation exposure levels in settlements located near uranium deposits and technogenic radioactive waste storage facilities [1, 16–18].

Investigations conducted at uranium legacy sites in Kyrgyzstan and Tajikistan have emphasized the need for systematic monitoring of radionuclide migration, gamma radiation, and radon-related radiation indicators [6, 19–22]. Similarly, studies performed at uranium legacy objects in China and in the Siwalik uranium mineralized zone of India have shown that the accumulation and migration of radionuclides in environmental components lead to an increase in radiation risk. The authors found that the activities of the ^{226}Ra, ^{232}Th, and ^{40}K radionuclides, as well as the radiological hazard indices, exceeded the world average values and emphasized the necessity of regular radioecological monitoring in such areas [7, 8].

Uzbekistan is one of the major uranium-producing countries in Central Asia. Uranium mining in this region began in 1958, and the Uchkuduk deposit played an important role in the development of the uranium industry. Subsequently, a large industrial infrastructure related to uranium ore mining, hydrometallurgical processing, and waste storage was established in this area. Since 1994, uranium in the Republic has been produced mainly by the in-situ leaching (ISL) method [23, 24].

Nevertheless, legacy sites from earlier conventional mining operations continue to pose potential radiological hazards to the surrounding environment and population. In Uzbekistan, studies carried out in the Yangiabad and Charkesar areas have likewise revealed gamma dose rates significantly exceeding natural background values in the areas of former uranium mines and waste rock dumps. In public buildings of Yangiabad, ^{222}Rn activity concentrations of 30–1050 Bq m^{-3} were recorded, with the annual effective dose reaching up to 7.6 mSv/year at some objects. Available reports also indicate approximately 500,000 m^3 of radioactive waste stored at Yangiabad and elevated uranium concentrations in water, reaching up to 1,312 ppb in mine discharge. These findings demonstrated that the migration of radionuclides into the environment under the influence of uranium legacy objects can continue for a long time [15, 25]. However, these studies have focused mainly on former uranium mines and uranium legacy objects. Relatively little data have been published on the radiation status of Uzbekistan's currently operating uranium mining and processing areas, in particular the Uchkuduk industrial zone.

As a result of many years of industrial activity, technogenic objects related to uranium mining and processing, including uranium mill tailings sites and production sections, have formed in the Uchkuduk area. This makes the area an important radioecological site for studying the environmental distribution of radionuclides, external gamma radiation, and the migration of radon and its decay products.

Previous radioecological studies in Uzbekistan have focused mainly on abandoned uranium legacy sites [15, 25], while the industrial zones of current uranium production remain poorly documented. Moreover, most studies report soil natural radioactivity, radon, or gamma dose rate separately [26–31]. Such data show where radionuclides are stored, but not whether they reach people. The soil inventory directly controls external gamma exposure, whereas inhalation exposure depends on radon exhalation, aerosol attachment, dust resuspension and atmospheric dilution, all of which can weaken the link between the source and the receptor. Whether the soil inventory of a uranium industry area can serve as a proxy for airborne exposure has therefore rarely been tested with co-located measurements.

This study addresses this question in the uranium industry area of Uchkuduk, Uzbekistan, where a uranium sorption recovery section, a 55 km^2 uranium mill tailings site, and a town of about 40,000 inhabitants [32] lie within 11 km of each other. At ten co-located points in each zone, we measured the specific activities of ^{226}Ra, ^{232}Th and ^{40}K in soil, $H^*(10)$, *EERC* and *LLAA*, and interpreted them together with wind data for the sampling days. The objectives were (i) to quantify the gradient of each indicator from the source zones to the residential area and (ii) to test whether the soil inventory predicts the airborne indicators within and between zones.

Materials and methods

Study area

The study area is located in the central part of Uzbekistan, in the Uchkuduk district of Navoi Region within the Central Kyzylkum uranium industry region. Sampling and measurements were carried out in the residential areas of Uchkuduk town, in the adjacent technogenic uranium mill tailings area located about 1 km south-east of the town, and at the uranium sorption recovery section situated about 11 km north-east of Uchkuduk. This town covers an area of approximately 10.27 km^2, the uranium mill tailings site 55 km^2, and the uranium sorption recovery section 4 km^2 (Fig. 1). The technogenic uranium mill tailings area consists mainly of a mixture of crushed rocks of granitic origin, clayey hydrometallurgical residues, and sandy-alluvial materials (Fig. 2).

The territory of Navoi Region, where Uchkuduk is located, is characterized by a sharply continental and semi-arid climate, with hot and dry weather in summer and relatively cold temperatures in winter. According to meteorological observations, the mean annual air temperature is approximately 15–16°C, and the annual precipitation is typically around 200 mm. Precipitation occurs mainly in the winter and spring months, while atmospheric precipitation is very rarely recorded during the summer season [33, 34].

Because Uchkuduk is adjacent to the storage area for uranium industry waste, ten control points were established throughout the town to monitor radionuclide migration into the environment and to monitor the radioecological status of the area. These control points are intended to compare the technogenically affected areas with the natural radiation background and to assess the spatial distribution of radionuclides. Soil samples were collected on 16 October 2025; *H** (10), *EERC* and *LLAA* were measured on 17–18 October 2025, *EERC* and *LLAA* between 09:00 and 16:00 local time. Hourly wind speed and direction at 10 m above ground level for Uchkuduk (~ 215 m a.s.l.) were obtained from the Open-Meteo Historical Weather API [35], based on the ECMWF IFS HRES model (9 km resolution), and cross-checked against ERA5 reanalysis [36]. On 17–18 October, wind speed ranged from 5.1 to 8.8 m s^{-1} (gusts up to 13.8 m s^{-1}), blowing continuously from the east (~ 76–90°). Wind was not recorded at the sampling points, and the model values refer to 10 m height, whereas sampling was at 1–1.5 m; the wind data are therefore used only for qualitative interpretation.

Quantification of natural radionuclides in the soils of the study area

Soil samples were collected from the surface (0–5 cm) layer at ten points in each of the residential area, the uranium mill tailings site, and the uranium sorption recovery section. All sampling points are shown in Fig. 1. Approximately 2 kg of soil was collected at each point using a plastic scoop, placed in polyethylene bags, and marked with dedicated labels.

Before laboratory analysis, the samples underwent preliminary treatment. Organic matter and small stones present in the soil samples were removed, and the samples were passed through a 5 mm sieve. The samples were first spread out and air-dried under ambient conditions, and then dried in an oven at 110°C for 24 h until a constant weight was achieved. The dried samples were placed in standard Marinelli plastic containers, hermetically sealed, and stored for 30 days. This period is considered sufficient for the establishment of secular equilibrium between ^{226}Ra and ^{232}Th and their short-lived decay products [37].

The specific activities of ^{226}Ra, ^{232}Th and ^{40}K were measured with an MKS-AT1315 gamma-beta spectrometer (ATOMTEX, Belarus) with a lead-shielded ø63 × 63 mm NaI(Tl) detector (50 keV–3 MeV; 1024 channels; resolution 8% at 662 keV; maximum permissible relative error ± 20%, P = 0.95) [38]. The instrument was within its annual metrological verification period. Energy calibration used a certified ^{228}Th point source (^{208}Tl, 2614.5 keV) and a certified ^{226}Ra

volume source (^{214}Pb, 242.0, 295.2 and 351.9 keV; ^{214}Bi, 609.3, 1120.3 and 1764.5 keV). Efficiency calibration used certified volume activity standards (OMASN) of ^{226}Ra, ^{232}Th, ^{40}K and ^{137}Cs in the same Marinelli geometry.

Because the NaI(Tl) resolution does not separate neighbouring lines of the uranium and thorium series (e.g. ^{214}Bi at 609.3 keV and ^{208}Tl at 583.2 keV), activities were not calculated from individual peak areas. Instead, each spectrum was decomposed by successive subtraction of density-normalised reference spectra of ^{232}Th, ^{226}Ra and ^{40}K recorded in the same geometry, which separates the contribution of each radionuclide to overlapping photopeaks and the Compton continuum; the expanded uncertainty of the decomposition is about 7% (k = 2) [30, 39]. Samples were counted for 2 h, the empty-container background was subtracted, and activities with expanded uncertainties (k = 2) were calculated with the ATWin software. The minimum detectable activities were about 10 Bq kg^{-1} for ^{226}Ra and ^{232}Th and 40 Bq kg^{-1} for ^{40}K [30].

The radium equivalent activity was calculated as [27, 40]:

$$\mathrm{Ra_{eq}}\left(\mathrm{Bq\,kg^{-1}}\right) = \mathrm{A_{Ra}} + 1.43\mathrm{A_{Th}} + 0.077\mathrm{A_K}$$

1

where A_{Ra}, A_{Th}, and A_K are the specific activities of ^{226}Ra, ^{232}Th, and ^{40}K, respectively [Bq kg^{-1}].

Measurement of ambient dose equivalent rate

The ambient dose equivalent rate of gamma radiation, *H**(10), in the study areas was measured using a DKS-96 dosimeter–radiometer (DOZA SPC, Russian Federation), which is designed for high-accuracy monitoring of ionizing radiation fields. The instrument is equipped with a scintillation detector and enables measurement of the radiation dose rate in the range from 0.1 μSv h^{-1} to 10 Sv h^{-1}. The integration time of the device is 1–60 s, and the measurement uncertainty does not exceed ± 12%.

Gamma dose rate was measured indoors and outdoors at the control points in the residential area and at the uranium sorption recovery section, but only outdoors at the uranium mill tailings site, where there are no buildings. Measurements were performed at ten points in each area at a height of 1 m above the ground surface. For the outdoor environment, *H**(10) values were measured up to five times within a circle of 5 m radius, while for the indoor environment, measurements were taken in several rooms of the building. The maximum and minimum values were adopted as an interval value [1, 17, 41].

Measurement of equilibrium equivalent radon concentration (EERC)

EERC was measured directly in indoor and outdoor air with an Alpharad Plus-AR automated radiometric complex (NTM-Zashchita Ltd., Russian Federation) [42]. The instrument draws air through an aerosol filter at 10 L min^{-1}, collects the aerosol-attached short-lived decay products of radon and thoron, and derives *EERC* from the alpha particles emitted by ^{218}Po and ^{214}Po on the filter. The *EERC* measurement range is 1.0–1.0 × 10^6 Bq m^{-3}, and the basic relative measurement uncertainty is ± 30%. Although the instrument also has a radon activity concentration unit, only *EERC* was recorded in this study; consequently, no equilibrium factor was assumed or applied.

Outdoors, the instrument was placed 1–1.5 m above the ground at locations away from buildings, walls, and other obstacles. At each point, two consecutive measurements were made in the EROA-10 mode (10-min sampling), and their mean was taken as the point value. Indoors, measurements were made in bedrooms and living rooms in the residential

area and in the operator and canteen rooms of the sorption recovery section, where personnel spend most of their working time. Doors and windows were kept closed for at least 30 min before and during sampling, and the instrument was positioned at breathing height (1–1.5 m), at least 0.5 m from walls and 1 m from ventilation sources [43]. A single EROA-5 measurement (5-min sampling) was made at each indoor point. Sampling followed the active filter-sampling principles of ASTM D6327-10 [44]. All *EERC* values are short-term (spot) measurements made between 09:00 and 16:00 local time and do not capture diurnal or seasonal variability.

Measurement of long-lived alpha activity (LLAA) of airborne aerosols

LLAA of airborne aerosols was determined by filter sampling followed by alpha radiometry [12]. Air was drawn for 16 min through three AFA-RSP-20 analytical aerosol filters (perchlorovinyl fibre; working area 20 cm^2) exposed simultaneously with a PU-3E/220 aspirator, with the sampler inlets 1 m above the ground (breathing height). The air volume was measured with the built-in mechanical counter of the aspirator (relative uncertainty ± 10%) and was 5 m^3. Because the inlets were at breathing height, locally resuspended dust is included by design, as it contributes to inhalation exposure. Each filter was measured separately, and the mean of the three filters was taken as the value for the sampling point.

After sampling, the filters were stored for at least 5 days so that the short-lived radon and thoron progeny decayed, leaving mainly long-lived alpha emitters. The alpha activity of each filter was measured in a fixed geometry with a Progress-AR alpha radiometer (DOZA SPC, Russian Federation) equipped with a 60 × 60 mm ZnS(Ag) scintillation detector (energy range 1.5–8 MeV; minimum detectable activity 9×10^{-3} Bq; relative measurement uncertainty ≤ 10%) [45]. The instrument was checked with standard control sources before the measurements, and the background was subtracted. *LLAA* was calculated as the alpha activity on the filters divided by the volume of sampled air and expressed in mBq m^{-3}.

The measured *LLAA* is a gross value, to which dust-borne long-lived alpha emitters of the uranium series (^{238}U, ^{234}U, ^{230}Th, ^{226}Ra, ^{210}Po) and atmospheric ^{210}Po formed from ^{222}Rn via ^{210}Pb can contribute [12, 13].

Statistical analysis

Statistical analysis and plotting were performed in Python 3.12 (Pandas, NumPy, Matplotlib and Seaborn). Relationships between the variables within each zone were evaluated with Spearman's rank correlation coefficient (ρ), which does not require normally distributed data and is robust to extreme values. With n = 10 per zone, correlations are significant at $p < 0.05$ when $|\rho| \geq 0.65$.

Results and discussion

Natural radionuclides and radium equivalent activity in soils

To assess the radiation characteristics of the soils in the study areas, the specific activities of the natural radionuclides ^{226}Ra, ^{232}Th, and ^{40}K were determined, and their distribution across the zones was analyzed. These radionuclides are the main natural sources of the terrestrial gamma radiation field, and their spatial variation in technogenically affected areas is important for characterizing the radioecological situation. The study covered three functionally distinct zones: the uranium sorption recovery technological section, the storage area for wastes generated from uranium ore processing, and the radiological monitoring points of the residential area.

The specific activities of ^{226}Ra, ^{232}Th, and ^{40}K in the soil samples and the Ra_{eq} values calculated from them are presented in Table 1.

Table 1

Specific activities of ^{226}Ra, ^{232}Th, and ^{40}K and calculated Ra_{eq} values in soil samples collected from the study areas

Sample code	^{226}Ra, Bq kg^{-1}	^{232}Th, Bq kg^{-1}	^{40}K, Bq kg^{-1}	Ra_{eq}, Bq kg^{-1}
Uranium sorption recovery section				
S1	204 ± 20	38 ± 4	620 ± 61	306.1
S2	57 ± 6	46 ± 5	926 ± 91	194.1
S3	212 ± 22	27 ± 3	618 ± 58	298.2
S4	94 ± 9	38 ± 5	667 ± 70	199.7
S5	198 ± 20	42 ± 5	605 ± 62	304.7
S6	146 ± 15	44 ± 4	820 ± 91	272.1
S7	95 ± 9	36 ± 4	985 ± 101	222.3
S8	120 ± 11	42 ± 5	890 ± 90	248.6
S9	146 ± 15	36 ± 4	720 ± 71	252.9
S10	187 ± 18	43 ± 5	740 ± 75	305.5
Uranium mill tailings site				
T1	2244 ± 210	173 ± 17	3025 ± 310	2724.3
T2	1804 ± 175	140 ± 15	2185 ± 209	2172.5
T3	2217 ± 223	78 ± 8	1465 ± 144	2441.3
T4	1182 ± 120	25 ± 3	238 ± 25	1236.1
T5	1110 ± 108	88 ± 9	1585 ± 160	1357.9
T6	1515 ± 152	25 ± 3	531 ± 52	1591.6
T7	2091 ± 203	54 ± 6	1238 ± 124	2263.5
T8	1718 ± 173	110 ± 12	398 ± 41	1905.9
T9	1984 ± 180	132 ± 11	855 ± 83	2238.6
T10	1355 ± 137	92 ± 10	642 ± 68	1536.0
Residential-area radiological monitoring points				
R1	32 ± 4	25 ± 3	422 ± 52	100.2
R2	45 ± 5	21 ± 3	536 ± 60	116.3
R3	56 ± 6	36 ± 5	752 ± 72	165.4
R4	56 ± 6	21 ± 3	685 ± 71	138.8
R5	36 ± 5	42 ± 5	644 ± 66	145.6
R6	23 ± 3	16 ± 3	741 ± 72	102.9
R7	53 ± 5	25 ± 4	856 ± 88	154.7

Sample code	^{226}Ra, Bq kg^{-1}	^{232}Th, Bq kg^{-1}	^{40}K, Bq kg^{-1}	Ra_{eq}, Bq kg^{-1}
Uranium sorption recovery section				
R8	52 ± 5	32 ± 3	653 ± 71	148.0
R9	63 ± 6	42 ± 4	563 ± 62	166.4
R10	42 ± 4	21 ± 3	485 ± 49	109.4

Uncertainties are expanded uncertainties (k = 2).

The results in Table 1 demonstrate a clear spatial differentiation of the natural radionuclide distribution among the study areas. In particular, the sharp inter-zonal differences observed in ^{226}Ra activity confirm that the long-term radiation impact of uranium mining and processing activity has persisted. The highest ^{226}Ra activities were recorded at the uranium mill tailings site, where values ran from 1110 to 2244 Bq kg^{-1}. These values are several times higher than the levels determined at the uranium sorption recovery section and tens of times higher than those at the monitoring points of the residential area, indicating a substantial accumulation of uranium-series radionuclides in the technogenic waste.

The high ^{226}Ra activity recorded at the uranium mill tailings site is associated with the retention and accumulation of radium in the waste materials after uranium extraction. For this reason, uranium tailings objects are often regarded as long-term sources of radiation hazard [3, 7].

At the uranium sorption recovery section, ^{226}Ra activity ranged from 57 to 212 Bq kg^{-1}. Although these values are higher than those in the residential area, they are considerably lower than at the tailings storage area, indicating an influence of the technological process, while the main accumulation of radionuclides is directly associated with the waste materials. At the monitoring points of the residential area, ^{226}Ra activity ranged from 23 to 63 Bq kg^{-1}, clearly reflecting the radiation gradient observed across the study areas. The consistent decrease in ^{226}Ra activity with increasing distance from the technogenic source demonstrates the direct link between the radionuclide distribution and the uranium industry objects and shows that their influence weakens with distance. Such a radiation gradient is characteristic of uranium mining and processing sites, and a decrease in radionuclide activity with increasing distance has also been reported at other uranium legacy sites [7].

For ^{232}Th, the highest activities were likewise recorded at the uranium mill tailings site, but its inter-zonal variation was much less than that of ^{226}Ra. This indicates that the radiation anomaly in the study area is associated mainly with the radionuclides of the uranium decay series and that ^{232}Th makes a more limited contribution to the overall radiological load. The wide range of variation of ^{40}K activity in all study areas shows that its distribution is governed not only by technogenic factors but also by the mineral composition and lithological characteristics of the soil-forming rocks. Consequently, the spatial variability of ^{40}K reflects the influence of uranium industry activity to a lesser extent than that of ^{226}Ra.

The highest Ra_{eq} values were also observed at the uranium mill tailings site. The Ra_{eq} values in this area, ranging from 1236.1 to 2724.3 Bq kg^{-1}, are primarily related to the sharp increase in ^{226}Ra activity and confirm the dominant role of the uranium-series radionuclides in shaping the external gamma radiation field [2]. Moreover, the fact that the Ra_{eq} values in all tailings samples exceed the internationally applied criterion of 370 Bq kg^{-1} several times over indicates a high potential for external radiation hazard in this area. Intermediate Ra_{eq} values were recorded at the uranium sorption recovery section, while the lowest values were observed at the monitoring points of the residential area. As a result, a

clear radiation gradient was formed among the three zones: residential-area monitoring points < uranium sorption recovery section < < uranium mill tailings site. This gradient shows that the impact of the uranium industry objects on the radioecological status of the environment decreases consistently with increasing distance.

To illustrate more clearly the statistical spread of the radionuclide activities and Ra_{eq} values across the zones, summary plots were constructed based on the minimum–maximum range, the mean value, and the mean ± standard deviation (Fig. 3).

**Horizontal lines represent the minimum–maximum range of values, colored blocks the mean ± standard deviation interval, and black vertical lines the mean value. A broken x-axis was used in the ^{226}Ra and Ra_{eq} plots to display the low- and high-value zones clearly within a single panel.*

Figure 3 summarizes the statistical distribution of the ^{226}Ra, ^{232}Th, ^{40}K, and Ra_{eq} values in the soil samples across the zones. The plots show that the uranium mill tailings site is characterized not only by the highest mean values of ^{226}Ra and Ra_{eq}, but also by the widest minimum-maximum ranges. This indicates that the radiation composition of the waste materials is not homogeneous and that the spatial distribution of the radionuclides is highly variable. This variability may be related to differences in the mineral composition of the waste materials, their emplacement history, and subsequent geochemical redistribution processes [3].

At the uranium sorption recovery section, the spread of the radionuclide and Ra_{eq} values was observed within comparatively narrower ranges, while the most stable statistical distribution was recorded at the monitoring points of the residential area. This result shows that the spatial variability of the radiation indicators decreases with increasing distance from the technogenic source.

The distribution characteristics observed for ^{232}Th and especially ^{40}K indicate that their spatial variability is governed not only by uranium industry activity but also by local geological and mineralogical factors [4]. Consequently, the statistical distribution of ^{40}K reflects the technogenic impact to a lesser extent than that of ^{226}Ra.

Overall, Fig. 3 not only demonstrates the radiation gradient among the study areas but also clearly reveals the internal spatial heterogeneity of the radionuclide distribution. However, the radionuclide activity in soil may not always be directly reflected in the airborne indicators or in *H**(10). Therefore, for a comprehensive assessment of the radioecological situation, the *H**(10), *EERC*, and *LLAA* indicators were analyzed separately in the following sections.

Ambient dose equivalent rate H*(10) across the studied areas and indoor–outdoor environments

While the radionuclide activities in soil and the Ra_{eq} values characterize the potential intensity of the radiation sources, the *H**(10) indicator makes it possible to assess how these sources manifest themselves in the external gamma radiation field. *H**(10) values were therefore analyzed for the three main study areas under outdoor and, where available, indoor conditions. Since the uranium mill tailings site was assessed as an open technogenic area, only outdoor *H**(10) values are presented for this area (Fig. 4). At each monitoring point, the *H**(10) value was expressed as the minimum-maximum interval recorded during the measurement.

In Fig. 4, the *H**(10) values are presented in interval form. The horizontal lines indicate the minimum-maximum *H**(10) range recorded during the measurements at each monitoring point. The markers on the lines represent the midpoint of this interval, i.e., the value $(H^*(10)_{min} + H^*(10)_{max})/2$. Blue circular markers and blue lines show the values under outdoor conditions, while orange square markers and orange lines show the values under indoor conditions. This approach allows *H**(10) to be assessed not as a single-point indicator but together with the variability range observed during the measurement.

The results in Fig. 4 show that *H*(10)* was highest at the uranium mill tailings site, where outdoor values ranged from 0.19 to 5.85 μSv h^{-1} and averaged about 1.75 μSv h^{-1} (mean of per-point midpoints, used for all sites). These levels agree with the ^{226}Ra and Ra_{eq} activities in Table 1 and suggest that gamma-emitting radionuclides in the waste materials contribute substantially to the external dose rate [1, 18]. The wide spread of values also points to a spatially uneven distribution of radioactive material within the tailings.

At the uranium sorption recovery section, outdoor *H*(10)* was 0.10–0.72 μSv h^{-1} (mean 0.28 μSv h^{-1}), compared with 0.06–0.35 μSv h^{-1} (mean 0.16 μSv h^{-1}) indoors. Lower indoor values imply that buildings partly shield external gamma radiation [17].

The lowest *H*(10)* was recorded at the monitoring points in the residential area, at 0.06–0.12 μSv h^{-1} outdoors (mean 0.086 μSv h^{-1}) and 0.04–0.11 μSv h^{-1} indoors (mean 0.078 μSv h^{-1}). The small difference between outdoor and indoor levels shows that external gamma radiation was nearly uniform here. Overall, *H*(10)* fell markedly with distance from the technogenic source [18].

Overall, a clear zonal gradient of the *H*(10)* values was observed: residential-area radiological monitoring points < uranium sorption recovery section < < uranium mill tailings site. This gradient is consistent with the results obtained for the soil radionuclides and Ra_{eq} and demonstrates the important contribution of the uranium-series radionuclides to the external gamma radiation. However, the fact that the indoor–outdoor differences did not manifest identically in all areas shows that the *H**(10) values are governed not only by the radionuclide inventory but also by factors such as local shielding, measurement geometry, and the spatial arrangement of the gamma sources [17].

Distribution of equilibrium equivalent radon concentration (EERC) across the studied areas

Figure 5 shows the distribution of the *EERC* values across the study areas. Outdoor and indoor measurements are available for the uranium sorption recovery section and the residential-area radiological monitoring points, allowing an assessment of the degree of accumulation of radon decay products in different environments. Since the uranium mill tailings site is an open technogenic area, only the outdoor *EERC* results are presented for this area.

**The lower and upper boundaries of the boxes represent the 25th–75th percentiles of the EERC values, respectively; the horizontal lines inside the boxes indicate the median values. The whiskers denote the minimum-maximum range of values. Outdoor and indoor measurements are distinguished by different colors.*

The box plots and summary statistics show clear differences in *EERC* between the studied areas, and between indoor and outdoor conditions. At the uranium sorption recovery section, outdoor *EERC* ranged from 7 to 31 Bq m^{-3} with a mean of 13.7 Bq m^{-3}. Indoors, it ranged from 12 to 46 Bq m^{-3} with a mean of 26.2 Bq m^{-3}. That makes the indoor mean about 1.9 times the outdoor one, which suggests radon decay products build up more readily in enclosed spaces. The likely reasons are weaker ventilation and the longer time radon progeny stay airborne inside buildings [10, 11].

At the tailings site, outdoor *EERC* (10–17 Bq m^{-3}; mean 13.6 Bq m^{-3}) was similar to that at the sorption section, although soil ^{226}Ra was about ten times higher. During the measurements, the wind blew steadily from the east at 5–9 m s^{-1} (at 10 m). Under such conditions, radon exhaled from the open tailings surface is rapidly diluted, so that the progeny concentration at breathing height depends more on atmospheric mixing than on the soil inventory [11].

At the radiological monitoring points of the residential area, outdoor *EERC* values were in the range of 4–8 Bq m^{-3}, with a mean of 5.7 Bq m^{-3}. Indoor values ranged from 7 to 17 Bq m^{-3}, with a mean value of 11.9 Bq m^{-3}. Thus, in this area, indoor *EERC* averaged about 2.1 times the outdoor level. This may be related to the more efficient accumulation and

longer retention of radon decay products in enclosed environments. As stated in the literature, the equilibrium factor for radon progeny is sensitive to ventilation intensity and aerosol conditions [11]; therefore, from a radioecological point of view, higher indoor than outdoor *EERC* values are an expected situation [17].

Overall, the *EERC* results do not repeat the same zonal gradient as *H**(10) and the soil radionuclides. While the highest *H**(10) values were observed at the uranium mill tailings site, relatively high *EERC* values were recorded under indoor conditions, particularly at the uranium sorption recovery section and the residential-area radiological monitoring points. This shows that *H**(10) is an integral dose indicator characterizing the external gamma radiation field, whereas *EERC* is sensitive to the accumulation and equilibrium state of radon progeny in the air environment [2].

The observed discrepancies indicate that the assessment of the airborne radiation hazard in uranium industry-affected areas should not be limited to *EERC* alone. Therefore, to characterize the radon progeny- and aerosol-related radiation hazards more fully, it is appropriate to apply additional indicators such as *LLAA* in combination.

Spatial variability and distribution of long-lived alpha activity (LLAA) in airborne aerosols

To assess the spatial distribution of *LLAA*, measurements were performed at the uranium sorption recovery section, the uranium mill tailings site, and the monitoring points of the residential area. The statistical distribution of the results is presented in Fig. 6.

The results obtained show differences in the *LLAA* values among the areas. The highest *LLAA* values were observed in the uranium sorption recovery section, with concentrations ranging from 7.61 to 31.2 mBq m^{-3} outdoors and from 3.1 to 12.6 mBq m^{-3} indoors. These high values may be associated with the dust generation and aerosol particle resuspension arising from technological activity. Previous studies have reported the occurrence of long-lived alpha-emitting radionuclides in respirable dust during uranium mining and processing, as well as their contribution to inhalation exposure [12].

At the tailings site, *LLAA* was measured outdoors only and ranged from 7.2 to 13.8 mBq m^{-3}, lower than at the sorption section although soil ^{226}Ra was about ten times higher. Given the dry conditions and wind gusts of up to 14 m s^{-1}, dust resuspension from the tailings surface cannot be excluded; the lower *LLAA* may instead reflect differences in the dust source and particle size between the zones, or the position of the sampling points relative to the dust plume. The strong correlation of *LLAA* with soil ^{226}Ra at this site (see below) supports a dust-borne origin.

In the residential area, *LLAA* was lowest (3.59–5.30 mBq m^{-3} outdoors and 2.8–4.3 mBq m^{-3} indoors), although on the sampling days the town lay downwind of the sorption section. This indicates strong dilution and deposition of the aerosol over the 11 km distance.

Relationships between soil radionuclides, airborne indicators and H*(10)

Spearman correlations within each zone were calculated using the soil activities, Ra_{eq}, outdoor *EERC* and *LLAA*, and the midpoints of the outdoor *H**(10) intervals (Fig. 7). With n = 10, only coefficients with $|\rho| \geq 0.65$ are significant at $p < 0.05$, and only these are interpreted.

In all zones, ^{226}Ra correlated strongly with Ra_{eq} (ρ = 0.91, 0.99 and 0.83 at the sorption section, tailings site and residential area, respectively), confirming that Ra_{eq} is controlled by ^{226}Ra. The airborne indicators, however, were linked to the soil in different ways. At the sorption section and in the residential area, outdoor *EERC* correlated with soil ^{226}Ra (ρ = 0.92 and 0.89) and Ra_{eq} (ρ = 0.83 and 0.78), whereas *LLAA* did not ($|\rho| \leq 0.30$). At the tailings site, the pattern was reversed: *LLAA* correlated with ^{226}Ra and Ra_{eq} (ρ = 0.92 and 0.91), while *EERC* did not ($|\rho| \leq 0.46$). Indoor *EERC* (not

shown in Fig. 7) also correlated with soil ^{226}Ra at the sorption section and in the residential area (ρ = 0.95 and 0.86). ^{40}K showed no significant correlation with the airborne indicators in any zone, and at the sorption section it was inversely related to ^{226}Ra (ρ = −0.74), indicating that its distribution is controlled mainly by the lithology of the soil-forming material rather than by technogenic input [46, 47].

The contrast between the zones suggests that, at points within built-up and industrial areas with moderate soil activity, local radon exhalation controls the progeny concentration at breathing height [11]. Over the open, wind-exposed tailings surface (5–9 m s^{-1} on the sampling days), radon is rapidly diluted, and the soil signal reaches the air mainly through resuspended dust, which carries long-lived alpha emitters of the uranium series [12, 13]. *H**(10) showed no significant correlation with any variable in any zone. This is expected because the interval midpoints reflect the source geometry within a 5 m radius, whereas each soil sample represents a single 0–5 cm point [2]. Given the small sample size and the single campaign, these relationships should be regarded as indicative.

Synthesis: from source to exposure pathway

Taken together, the results show that the three zones differ not only in the magnitude of the source but also in the pathway by which it can reach people.

Tailings site: highest inventory, strongest external gamma radiation. Soil ^{226}Ra (1110–2244 Bq kg^{-1}) and *H**(10) (up to 5.85 μSv h^{-1}) were highest here, but outdoor *EERC* was no higher than at the sorption section, and *LLAA* was lower. The hazard on the site is therefore expressed mainly by external gamma radiation, while the soil signal reaches the air mainly through dust, as indicated by the correlation of *LLAA* with soil ^{226}Ra. The tailings site lies about 1 km south-east of the town. On the sampling days, the easterly wind carried air from the tailings past the southern edge of the town rather than over it; the transport of tailings-derived radon and dust towards the town under south-easterly winds could therefore not be assessed.

Sorption recovery section: moderate inventory, highest airborne indicators. Soil ^{226}Ra was an order of magnitude lower than at the tailings site, yet outdoor *LLAA* was the highest of all zones, and indoor *EERC* in the operator and canteen rooms reached 46 Bq m^{-3}. Technological dust and the accumulation of radon progeny in occupied rooms indicate that inhalation deserves particular attention for workers in this zone.

Residential area: background conditions. All indicators were close to natural background levels, although the town lay downwind of the sorption section on the sampling days. Mean outdoor *LLAA* was about four times lower than at the section, indicating strong dilution and deposition of the aerosol over the 11 km distance. Indoor *EERC* (7–17 Bq m^{-3}) was about twice the outdoor value and is controlled mainly by building ventilation.

Implications for monitoring. Because neither the soil inventory nor *H**(10) predicted the airborne indicators, monitoring based only on gamma surveys and soil sampling may underestimate the inhalation hazard where the source is moderate, but dust generation is high, as at the sorption section. Direct measurement of *EERC* and *LLAA*, including in occupied rooms, should therefore be part of routine monitoring in uranium industry areas.

International comparison of radiological parameters in uranium-affected areas

As shown in Table 2, soil ^{226}Ra at the Uchkuduk tailings site (1110–2244 Bq kg^{-1}) is of the same order as in the contaminated areas of South Kazakhstan, 2350 Bq kg^{-1} [1], but much lower than in uranium tailings reservoirs in China, 8270–16060 Bq kg^{-1} [7]. Ra_{eq} at the tailings site (1236–2724 Bq kg^{-1}) exceeded the 370 Bq kg^{-1} criterion at all points

and was higher than the values reported for North-East Kazakhstan, 64.8–717.4 Bq kg^{-1} [18], and the Liṣava uranium mining sector, 118.33–458.31 Bq kg^{-1} [48]. The maximum *H**(10) at the tailings site (5.85 μSv h^{-1}) is about 70–100 times the world average values of 0.059–0.084 μSv h^{-1} [2] but lower than the maxima reported for Taboshar and Digmai [20]. *EERC* in all Uchkuduk zones (up to 46 Bq m^{-3} indoors) was in the lower part of the ranges reported for settlements near uranium mining areas in Kazakhstan: 1–191 Bq m^{-3} [1] and 18–4974 Bq m^{-3} [16]. *LLAA* was not included in the comparison, because the sampling and reporting methods in the literature are not standardised. Overall, the Uchkuduk area falls within the range of other Central Asian uranium industry areas and below the most contaminated sites.

Table 2
Comparison of the radiological indicators of the Uchkuduk uranium industry areas with other uranium industry and legacy areas

Study area	^{226}Ra (Bq kg^{-1})	^{232}Th (Bq kg^{-1})	^{40}K (Bq kg^{-1})	Ra_{eq} (Bq kg^{-1})	*EERC* (Bq m^{-3})		*H**(10) (μSv h^{-1})		References
					Outdoor	*Indoor*	*Outdoor*	*Indoor*	
Uranium sorption recovery section	57–212	27–46	605–985	194.1–306.1	7–31	12–46	0.1–0.72	0.06–0.35	This study
Uranium mill tailings site	1110–2244	25–173	238–3025	1236.1–2724.3	10–17		0.19–5.85		This study
Uchkuduk residential area	23–63	16–42	422–856	100.2–166.4	4–8	7–17	0.06–0.12	0.04–0.11	This study
South Kazakhstan, contaminated area	2350	270	860				0.5–1.2		[1]
South Kazakhstan, residential areas						1–191	0.03–0.1	0.04–0.15	[1]
Northern Kazakhstan uranium mining settlements						18–4974	0.56 ± 0.19	0.4 ± 0.13	[16]
North-East Kazakhstan, mothballed uranium mining facility	63–97	60–200	670–1400	64.8–717.4			0.1–0.9	0.3–3.5	[18]
Taboshar and Digmai uranium legacy sites, Tajikistan					16–1280	15–830	0.3–22.1	0.1–1.3	[20]
Lișava uranium mining sector, Romania	32.12–396.23[c]	7.23–48.16	497.32–615.32	118.33–458.31			0.058–0.215[b]		[48]
Uranium tailings reservoir, China	8270–16060	700–1580	2890–8600				0.119–0.624[b]	0.412–0.979[b]	[7]
World average	35	30	400	-	6[a]	16[a]	0.059[b]	0.084[b]	[2]

[a] *EERC calculated from the world average radon concentrations of 10 Bq m^{-3} (outdoor) and 40 Bq m^{-3} (indoor) with equilibrium factors of 0.6 and 0.4* [2]. [b] *Estimated from the absorbed gamma dose rate in air assuming 1 nGy h^{-1} ≈ 1 nSv h^{-1}; for the world average, from 59 and 84 nGy h^{-1}* [2]. [c] *Reported as ^{238}U. The Ra_{eq} value of 370 Bq kg^{-1} is a recommended upper limit, not an average* [40].

Limitations

This study has several limitations. The data come from a single campaign (16–18 October 2025), and EERC and LLAA were short-term daytime measurements, so they cannot describe diurnal or seasonal variability. Because convective mixing is strongest during the day, outdoor EERC may also be lower than the daily mean. In addition, radon was measured as LLAA gross alpha activity, and since the filters were not kept, individual alpha emitters could not be identified. Finally, the vertical distribution of radionuclides in soil was not studied, and with n = 10 per zone, the correlation analysis has limited statistical power.

Conclusions

(1) The uranium mill tailings site is the main radiation source in the Uchkuduk area: ^{226}Ra (1110–2244 Bq kg^{-1}), Ra_{eq} (1236–2724 Bq kg^{-1}, above the 370 Bq kg^{-1} criterion at all points) and $H^*(10)$ (up to 5.85 μSv h^{-1}) decreased sharply towards the sorption section and the residential area.

(2) The airborne indicators did not follow this gradient. *LLAA* was highest at the sorption section, and *EERC* was highest indoors in the occupied rooms of the section and the town. The soil inventory and $H^*(10)$ therefore cannot be used as proxies for the inhalation hazard.

(3) The link between soil and air depended on the zone: *EERC* followed soil ^{226}Ra at the sorption section and in the residential area, whereas at the wind-exposed tailings site the soil signal was carried mainly by dust (*LLAA*).

(4) In the residential area, all indicators were close to natural background levels on the sampling days. Repeated measurements including night-time, seasonal and south-easterly wind conditions, together with alpha-spectrometric analysis of aerosol filters, are needed to quantify the transport of radon and dust from the tailings to the town.

Declarations

Ethical approval

Not applicable.

Consent to participate

Not applicable.

Consent for publication

Not applicable.

Competing interests

The authors declare no competing interests.

Funding

This research received no external funding.

Author Contribution

Author contribution U.H., A.M., G.Al., M.Q. and G.As. performed the material preparation and data collection. U.H., A.M., D.K. and S.S. performed the data analysis. U.H. prepared the figures. U.H. and A.M. wrote the main manuscript text. A.M. supervised the study. All authors reviewed and approved the final manuscript.

Availability of data and materials

The datasets generated during the current study are available from the corresponding author upon reasonable request.

Code availability

Not applicable.

References

1. 1. Bakhtin M, Ibrayeva D, Kashkinbayev Y, et al (2025) Environmental Monitoring in Uranium Deposit and Indoor Radon Survey in Settlements Located near Uranium Mining Area, South Kazakhstan. Atmosphere 16:536. https://doi.org/10.3390/atmos16050536
2. 2. UNSCEAR (2000) Sources and Effects of Ionizing Radiation: UNSCEAR 2000 Report to the General Assembly, with Scientific Annexes. Volume I: Sources. United Nations, New York
3. 3. IAEA (2002) Monitoring and Surveillance of Residues from the Mining and Milling of Uranium and Thorium. International Atomic Energy Agency, Vienna, Austria
4. 4. Tye AM, Milodowski AE, Smedley PL (2017) Distribution of Natural Radioactivity in the Environment. British Geological Survey, Nottingham, UK
5. 5. UNSCEAR (2010) Sources and Effects of Ionizing Radiation: UNSCEAR 2008 Report to the General Assembly, with Scientific Annexes. Volume I: Sources. United Nations, New York
6. 6. Egemberdieva AD, Kamchybekova KD, Mamaturaimova NA, et al (2025) Radiation Pollution and Public Health Impacts in Mailuu-Suu, Kyrgyzstan. Journal of Environmental & Earth Sciences 7:363–375. https://doi.org/10.30564/jees.v7i8.10588
7. 7. Liu Y, Zhou W, Gao B, et al (2021) Determination of radionuclide concentration and radiological hazard in soil and water near the uranium tailings reservoir in China. Environmental Pollutants and Bioavailability 33:174–183. https://doi.org/10.1080/26395940.2021.1951123
8. 8. Pandit P, Mangala P, Saini A, et al (2020) Radiological and pollution risk assessments of terrestrial radionuclides and heavy metals in a mineralized zone of the siwalik region (India). Chemosphere 254:126857. https://doi.org/10.1016/j.chemosphere.2020.126857

9. 9. Eisenbud M, Gesell T (1997) Environmental Radioactivity: From Natural, Industrial, and Military Sources, 4th ed. Academic Press, Cambridge, MA, USA
10. 10. Kreuzer M, McLaughlin J (2010) Radon. In: WHO Guidelines for Indoor Air Quality: Selected Pollutants. World Health Organization, Geneva
11. 11. Vogiannis EG, Nikolopoulos D (2015) Radon Sources and Associated Risk in Terms of Exposure and Dose. Front Public Health 2:. https://doi.org/10.3389/fpubh.2014.00207
12. 12. Jha S, Ghosh DK, Mishra UC (2000) Assessment of exposure of miners to the α-rays of long-lived radionuclides associated with respirable ore dust in the Jaduguda U mine. Journal of Environmental Radioactivity 48:317–326. https://doi.org/10.1016/S0265-931X(99)00078-8
13. 13. Baskaran M (2011) Po-210 and Pb-210 as atmospheric tracers and global atmospheric Pb-210 fallout: a Review. Journal of Environmental Radioactivity 102:500–513. https://doi.org/10.1016/j.jenvrad.2010.10.007
14. 14. Terray L, D'Amico D, Masson O, Sabroux J-C (2020) What can gross alpha/beta activities tell about 210Po and 210Pb in the atmosphere? Journal of Environmental Radioactivity 225:106437. https://doi.org/10.1016/j.jenvrad.2020.106437
15. 15. Stegnar P, Shishkov I, Burkitbayev M, et al (2013) Assessment of the radiological impact of gamma and radon dose rates at former U mining sites in Central Asia. Journal of Environmental Radioactivity 123:3–13. https://doi.org/10.1016/j.jenvrad.2012.12.005
16. 16. Kashkinbayev Y, Ibrayeva D, Aumalikova M, et al (2025) Radon Concentration Survey in Settlements Located in Uranium Mining Territory in Northern Kazakhstan. IJERPH 22:723. https://doi.org/10.3390/ijerph22050723
17. 17. Lesbek A, Omori Y, Bakhtin M, et al (2025) Seasonal Variations in Effective Radiation Dose in Residential Buildings of the Akmola Region: Assessing the Impact of Basement Presence and Proximity to Uranium Tailings. Environments 12:357. https://doi.org/10.3390/environments12100357
18. 18. Subbotin S, Krivitskiy P, Larionova N, et al (2025) Assessment of the radiological situation near a mothballed uranium mining facility in North-East Kazakhstan. Sci Rep 15:16426. https://doi.org/10.1038/s41598-025-01697-6
19. 19. Corcho Alvarado JA, Balsiger B, Röllin S, et al (2014) Radioactive and chemical contamination of the water resources in the former uranium mining and milling sites of Mailuu Suu (Kyrgyzstan). Journal of Environmental Radioactivity 138:1–10. https://doi.org/10.1016/j.jenvrad.2014.07.018
20. 20. Lespukh E, Stegnar P, Yunusov M, et al (2013) Assessment of the radiological impact of gamma and radon dose rates at former U mining sites in Tajikistan. Journal of Environmental Radioactivity 126:147–155. https://doi.org/10.1016/j.jenvrad.2013.07.019
21. 21. Mirsaidov U, Nazarov KM, Tillozoda HI, et al (2026) Ways to reduce the risk of radioactive contamination at the Digmay tailing pond in Tajikistan. Ecol Eng Environ Technol 27:424–430. https://doi.org/10.12912/27197050/217565
22. 22. Severinenko MA, Solodukhin VP, Djenbaev BM, et al (2023) Occurrence of Radionuclides and Hazardous Elements in the Transboundary River Basin Kyrgyzstan–Kazakhstan. Water 15:1759. https://doi.org/10.3390/w15091759
23. 23. IAEA (1997) Changes and Events in Uranium Deposit Development, Exploration, Resources, Production and the World Supply-Demand Relationship. International Atomic Energy Agency, Vienna
24. 24. Navoiyuran State Enterprise Company History. In: Navoiyuran State Enterprise. https://navoiyuran.uz/en/about-us/. Accessed 31 May 2026
25. 25. Tsukatani T, Toderich K, Goldstein RI (2008) Uranium mine aftermath and Yangiabad Expedition in Uzbekistan. Kyoto University, Institute of Economic Research, Kyoto, Japan

26. 26. Allaberganova G, Pulatov X, Urunov I, Muzafarov A (2023) Factors increase in background radiation at uranium production facilities. E3S Web Conf 417:01007. https://doi.org/10.1051/e3sconf/202341701007
27. 27. Khasanov S, Tukhtaev U, Mamatkulov O, et al (2024) Natural radionuclide profiles and radiological risks in soils and rocks of the Koytash–Ugam Range, Uzbekistan. Environ Monit Assess 196:847. https://doi.org/10.1007/s10661-024-13015-0
28. 28. Muzafarov AM, Oslopovskiy SA, Sattarov GS (2016) Radiometric investigations of technogenic objects. tsm 15–19. https://doi.org/10.17580/tsm.2016.02.02
29. 29. Safarov A, Safarov A, Khasanov S, et al (2023) Evaluation of radon hazards at the rural settlements of Uzbekistan. Environ Monit Assess 195:915. https://doi.org/10.1007/s10661-023-11493-2
30. 30. Tukhtaev U, Khasanov S, Safarov A, Proshad R (2023) Assessment of radioactivity of the Sobirsoy reservoir and adjacent areas of the Nurabad district, Uzbekistan. Radiochimica Acta 111:781–791. https://doi.org/10.1515/ract-2023-0153
31. 31. Tukhtaev U, Khasanov S, Fayzullayev J, et al (2024) Determination of natural radionuclides and heavy metal concentrations in the groundwater and adjacent areas of the Kattakurgan reservoir, Uzbekistan. Radiochimica Acta 112:127–137. https://doi.org/10.1515/ract-2023-0254
32. 32. National Statistics Committee of the Republic of Uzbekistan (2026) TOP-10 lowest-populated districts and cities. Tashkent
33. 33. Kulmatov R, Groll M, Rasulov A, et al (2018) Status quo and present challenges of the sustainable use and management of water and land resources in Central Asian irrigation zones - The example of the Navoi region (Uzbekistan). Quaternary International 464:396–410. https://doi.org/10.1016/j.quaint.2017.11.043
34. 34. World Bank Group (2020) Climatology Data (1991–2020). In: Climate Change Knowledge Portal. https://climateknowledgeportal.worldbank.org. Accessed 31 May 2026
35. 35. Zippenfenig P (2024) Open-Meteo.com Weather API
36. 36. Hersbach H, Bell B, Berrisford P, et al (2020) The ERA5 global reanalysis. Quart J Royal Meteoro Soc 146:1999–2049. https://doi.org/10.1002/qj.3803
37. 37. IAEA (1989) Measurement of Radionuclides in Food and the Environment: A Guidebook. International Atomic Energy Agency, Vienna, Austria
38. 38. ATOMTEX (2020) MKS-AT1315 Gamma-Beta Spectrometer: Technical Specifications. ATOMTEX, Minsk, Belarus
39. 39. Azimov AN, Hushmuradov SK, Muminov IT, et al (2008) Gamma-spectrometric determination of natural radionuclides and 137Cs concentrations in environmental samples: the improved scintillation technique. Radiation Measurements 43:66–71
40. 40. Beretka J, Mathew PJ (1985) Natural Radioactivity of Australian Building Materials, Industrial Wastes and By-products: Health Physics 48:87–95. https://doi.org/10.1097/00004032-198501000-00007
41. 41. Yılmazkaya İ, Altinsoy N, Şimşek V (2025) Radiologic risk assessment of outdoor gamma dose rate in Çorum province, Turkey. J Radioanal Nucl Chem 334:6633–6639. https://doi.org/10.1007/s10967-025-10023-3
42. 42. NTM-Zashchita Ltd. (2012) Alpharad Plus-AR: Measuring Complex for Monitoring Radon, Thoron and Their Daughter Products. NTM-Zashchita Ltd., Moscow, Russia
43. 43. Puchkov AV, Berezina EV, Yakovlev EYu, et al (2022) Radon Flux Density In Conditions Of Permafrost Thawing: Simulation Experiment. GES 15:5–18. https://doi.org/10.24057/2071-9388-2022-023
44. 44. ASTM International (2016) Standard Test Method for Determination of Radon Decay Product Concentration and Working Level in Indoor Atmospheres by Active Sampling on a Filter. ASTM International, West Conshohocken, PA

45. 45. Nazarov Z, Allaberganova G, Pulatov K, Muzafarov A (2023) Radiometric measurements at uranium mined-out sitesbefore their reclamation. XXI century Technosphere Safety 8:407–414. https://doi.org/10.21285/2500-1582-2023-4-407-414
46. 46. Forkapic S, Vasin J, Bikit I, et al (2017) Correlations between soil characteristics and radioactivity content of Vojvodina soil. Journal of Environmental Radioactivity 166:104–111. https://doi.org/10.1016/j.jenvrad.2016.04.003
47. 47. Menshikova E, Perevoshchikov R, Belkin P, Blinov S (2021) Concentrations of Natural Radionuclides (40K, 226Ra, 232Th) at the Potash Salts Deposit. J Ecol Eng 22:179–187. https://doi.org/10.12911/22998993/132544
48. 48. Ion A, Cosac A, Ene VV (2022) Natural Radioactivity in Soil and Radiological Risk Assessment in Lișava Uranium Mining Sector, Banat Mountains, Romania. Applied Sciences 12:12363. https://doi.org/10.3390/app122312363

Figures

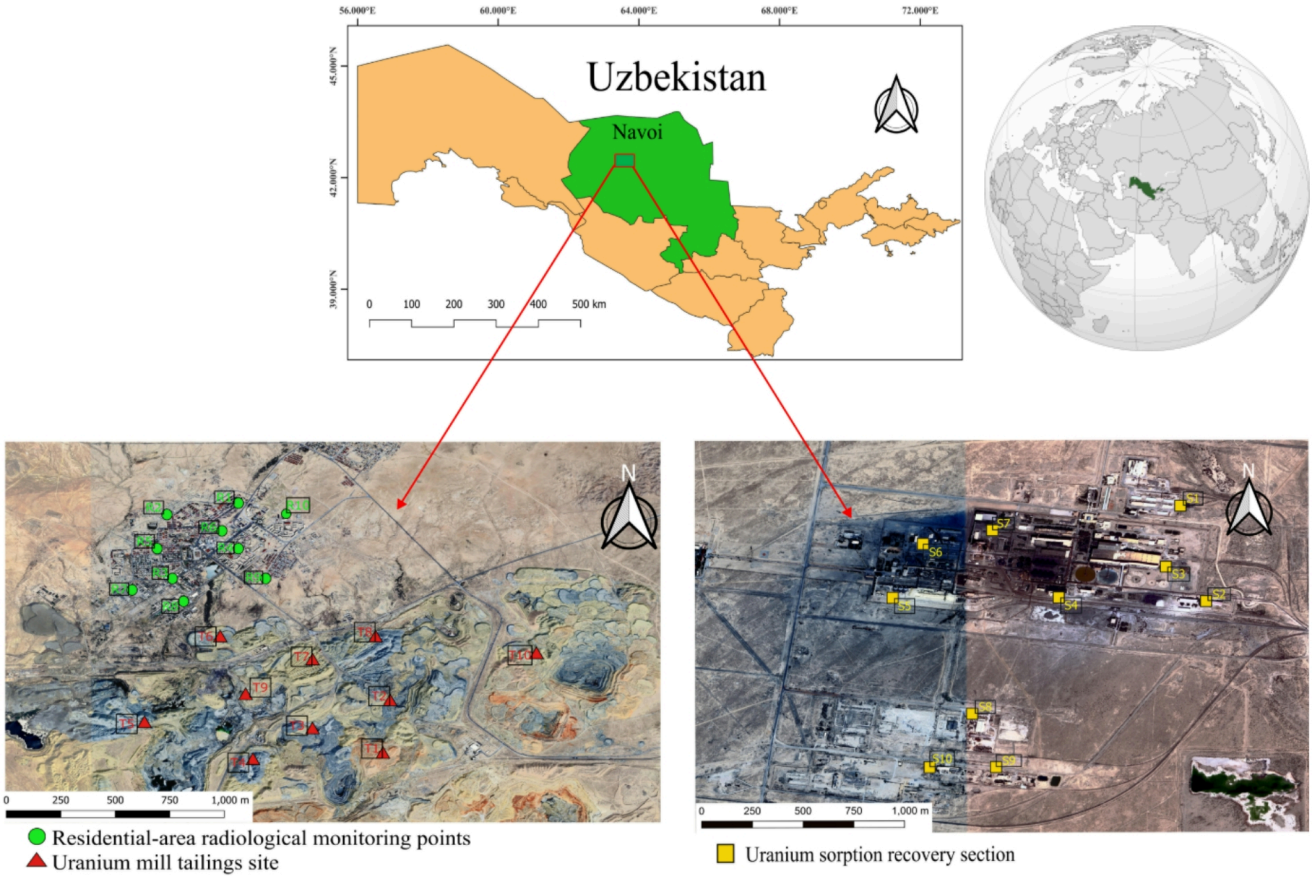


Figure 1

Map of the study area and locations of sampling sites



Figure 2

Uranium mill tailings site

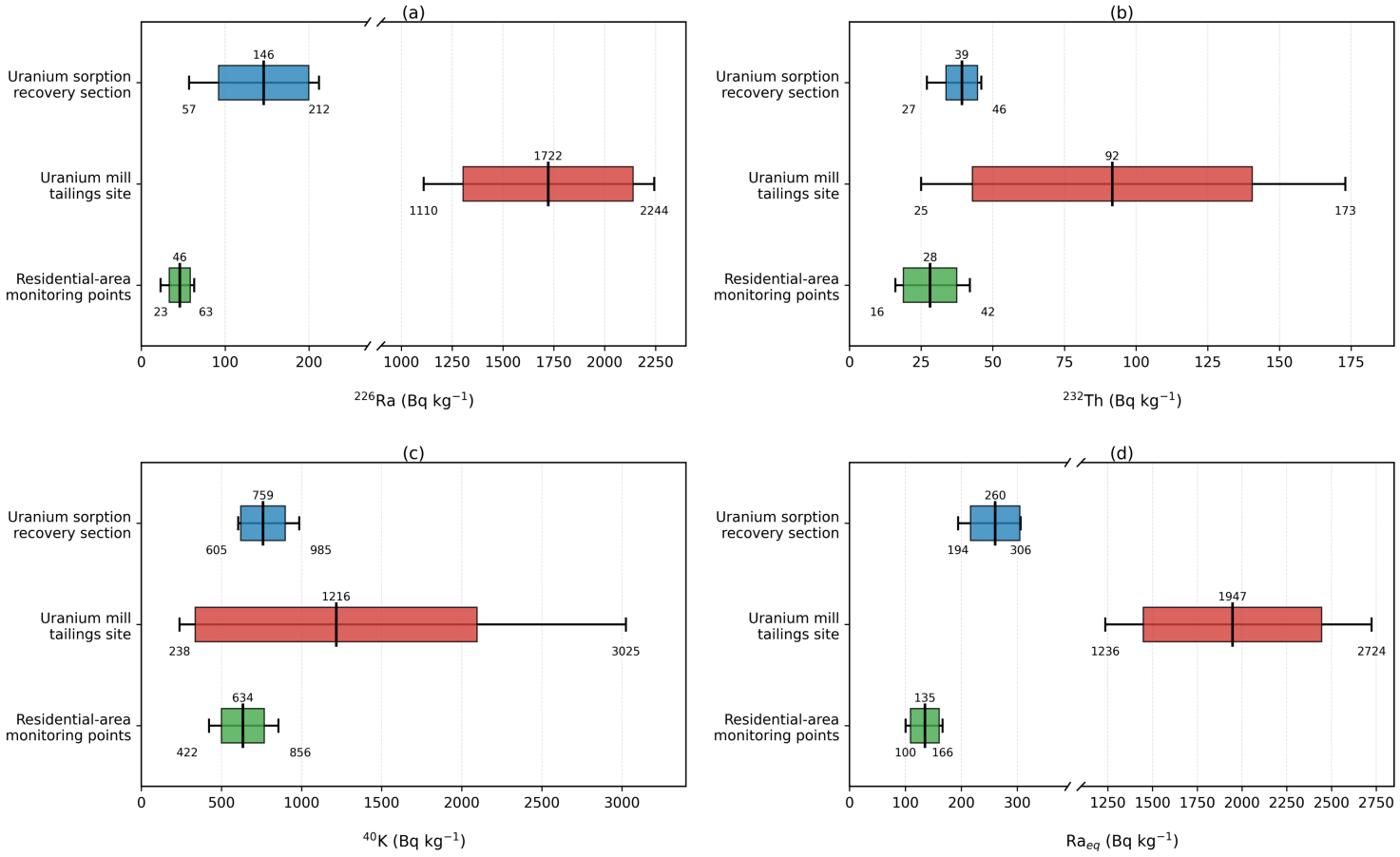


Figure 3

Statistical distribution of natural radionuclide and Ra_{eq} activities in soil samples across the study zones*

Horizontal lines represent the minimum–maximum range of values, colored blocks the mean ± standard deviation interval, and black vertical lines the mean value. A broken x-axis was used in the ^{226}Ra and Ra_{eq} plots to display the low- and high-value zones clearly within a single panel.

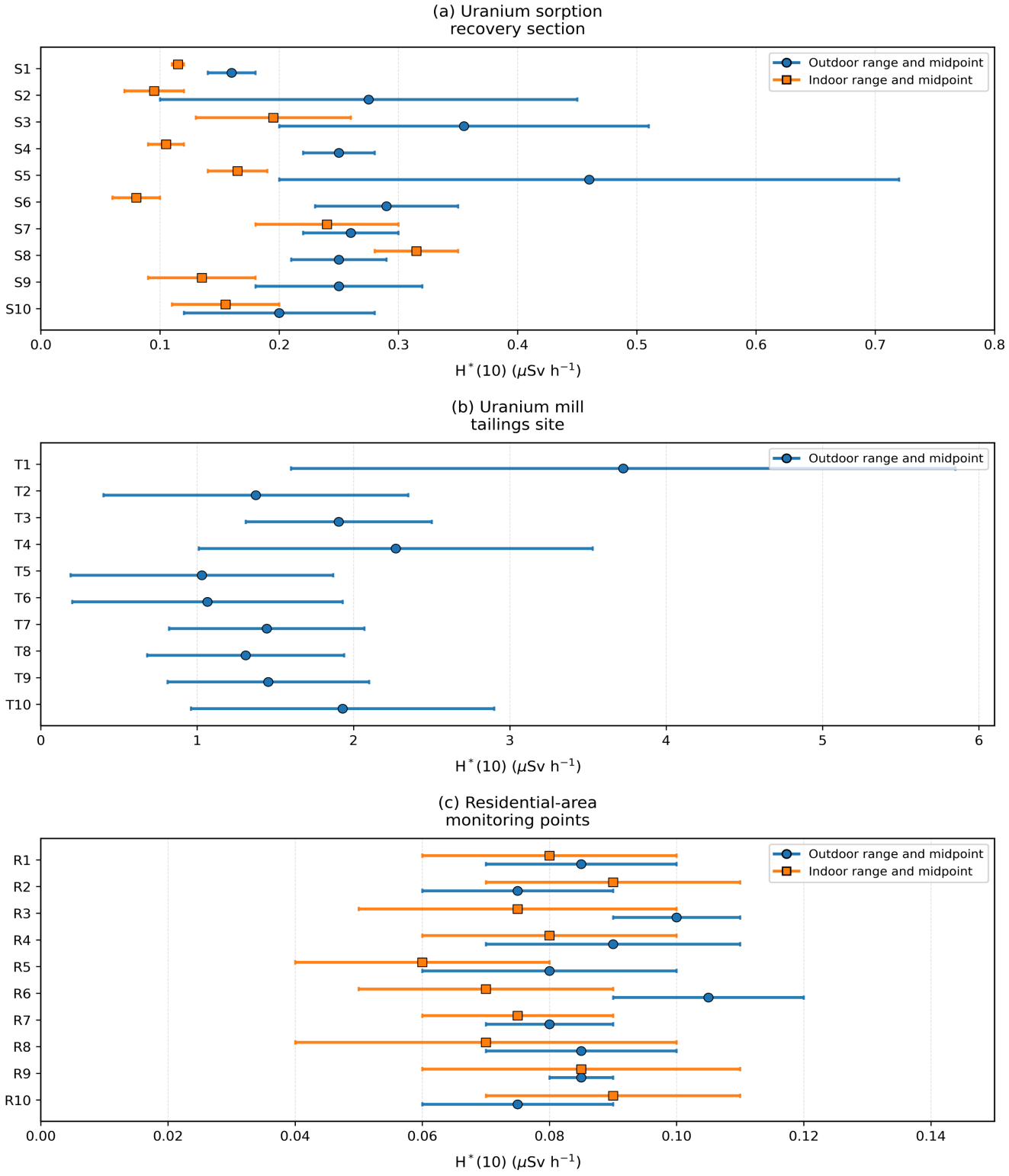


Figure 4

Minimum–maximum ranges of ambient dose equivalent rate *H**(10) under outdoor and indoor conditions across the studied areas

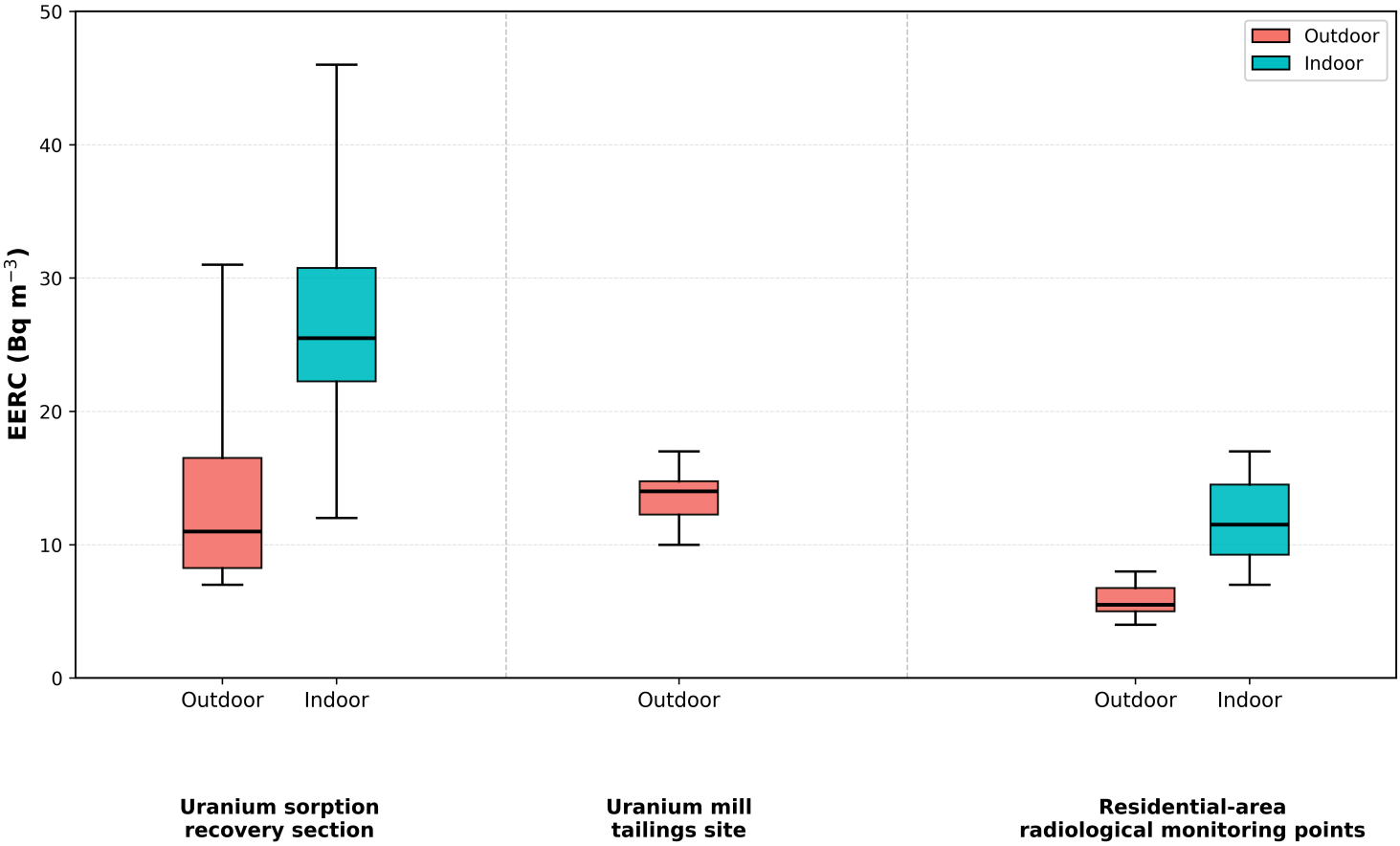


Figure 5

Distribution of the equilibrium equivalent radon concentration (*EERC*) under outdoor and indoor conditions across the study areas*

**The lower and upper boundaries of the boxes represent the 25th–75th percentiles of the EERC values, respectively; the horizontal lines inside the boxes indicate the median values. The whiskers denote the minimum-maximum range of values. Outdoor and indoor measurements are distinguished by different colors.*

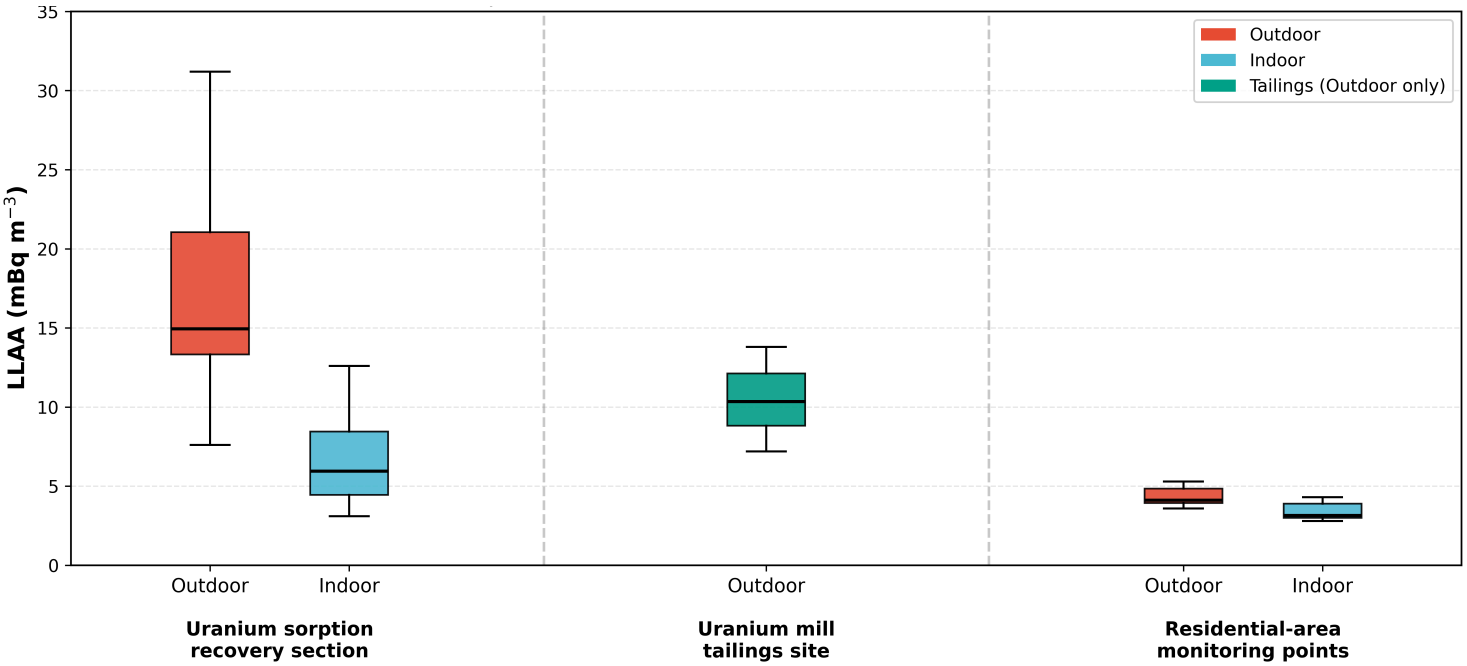


Figure 6

Spatial distribution of long-lived alpha activity (*LLAA*) across the studied areas

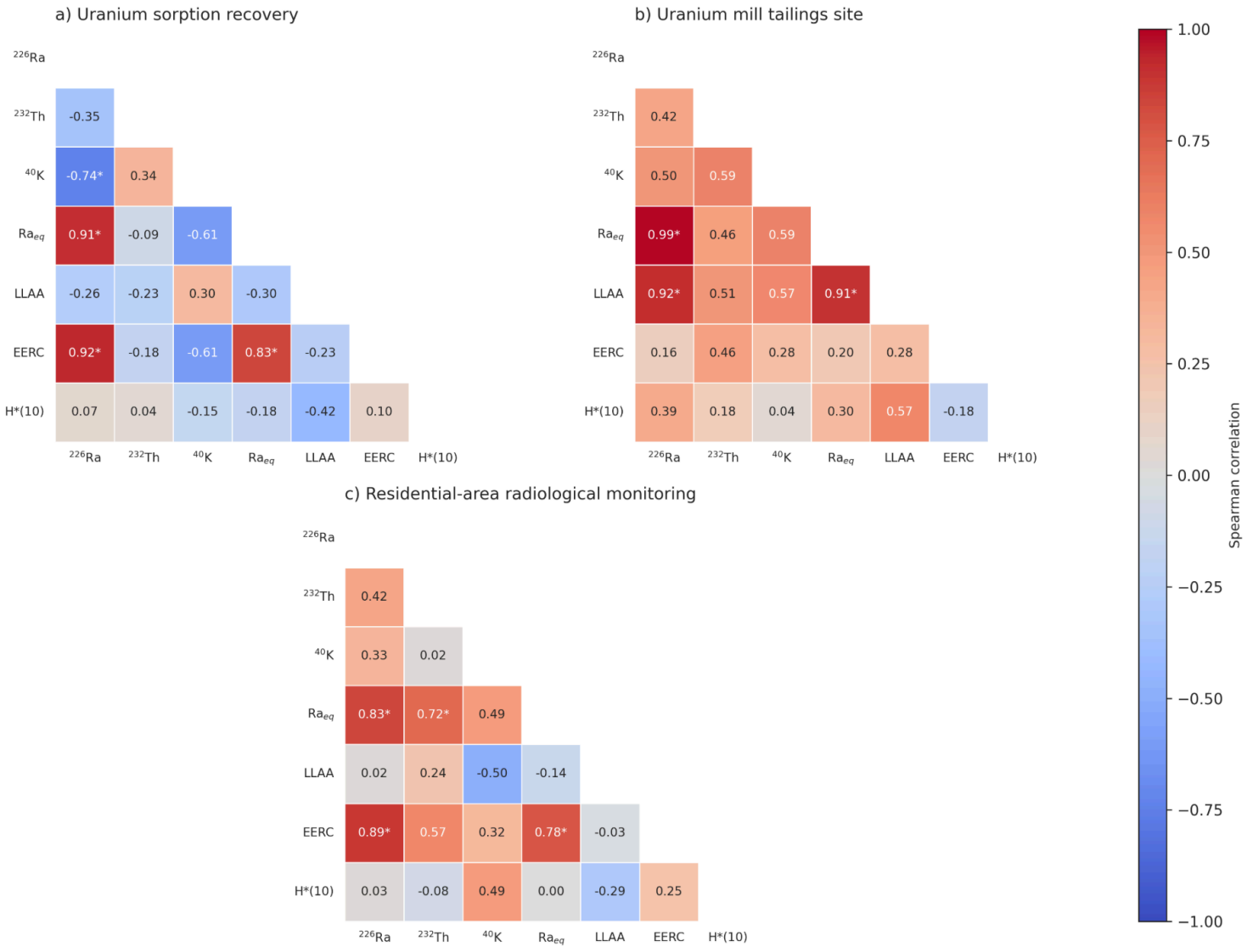


Figure 7

Spearman correlation matrices between soil radionuclides (^{226}Ra, ^{232}Th, ^{40}K), Ra_{eq}, airborne indicators (outdoor *EERC* and *LLAA*) and *H**(10) (interval midpoints) for (a) the uranium sorption recovery section, (b) the uranium mill tailings site and (c) the residential area (n = 10 per zone). Coefficients marked with an asterisk are significant at $p < 0.05$ ($|\rho| \geq 0.65$)